

Growth dynamics underlying petal shape and asymmetry

Anne-Gaëlle Rolland-Lagan^{*†}, J. Andrew Bangham^{*} & Enrico Coen[†]

^{*} School of Information Systems, UEA, Norwich, NR4 7TJ, UK

[†] John Innes Centre, Norwich Research Park Colney, Norwich, NR4 7UH, UK

Development commonly involves the generation of complex shapes from simpler ones. One way of following this process is to use landmarks to track the fate of particular points in a developing organ^{1–7}, but this is limited by the time over which it can be monitored. Here we use an alternative method, clonal analysis⁸, whereby dividing cells are genetically marked and their descendants identified visually, to observe the development of *Antirrhinum* (snapdragon) petals. Clonal analysis has previously been used to estimate growth parameters of leaves^{9–11} and *Drosophila* wings^{12–14} but these results were not integrated within a dynamic growth model. Here we develop such a model and use it to show that a key aspect of shape—petal asymmetry—in the petal lobe of *Antirrhinum* depends on the direction of growth rather than regional differences in growth rate. The direction of growth is maintained parallel to the proximodistal axis of the flower, irrespective of changes in shape, implying that long-range signals orient growth along the petal as a whole. Such signals may provide a general mechanism for orienting growth in other growing structures.

The transformations in shape of a growing structure depend on the growth properties of its component regions. For each region and time point, these properties can be conveniently captured by three

types of parameter: the rate of increase in size (growth rate), the degree to which growth occurs preferentially in any direction (anisotropy) and the angle at which the principal direction of growth is oriented relative to an underlying coordinate system (direction) (Fig. 1a). These parameters can vary both in space (that is, between regions) and time, so there are potentially many different ways, with varying degrees of complexity, by which one shape can be transformed into another. Describing the growth of any structure therefore requires parameters to be determined experimentally. Because growth is a complex spatiotemporal problem, the quantitative contribution of these parameters can only be evaluated effectively by incorporating them within a dynamic growth model. This can establish whether the parameters are sufficient to account for the observed shape changes and allows the contribution of each parameter to be explored.

One problem when using clonal analysis to measure growth parameters is that the orientation of growth cannot be inferred simply from the final clone shape¹⁵ because the internal coordinate system of the organ will often be deformed by growth. Relating a mature clone to its growth orientation at the time of initiation can only be done when this deformation is known. We have compared clones induced at successive times during development to determine growth parameters together with the sequence of deformations of a superimposed grid. The method is applied by working backward from the final shape. The organ is subdivided into a grid of regions interconnected by 'springs' with resting lengths initially set according to the shape of the mature organ. Growth parameters just before cell divisions stop are then calculated for each region, on the basis of comparisons of clones induced late in development (Fig. 1b–e). The resting lengths of the springs are then adjusted according to these parameters, allowing each region to shrink, as the springs 'relax', to generate a revised grid and the

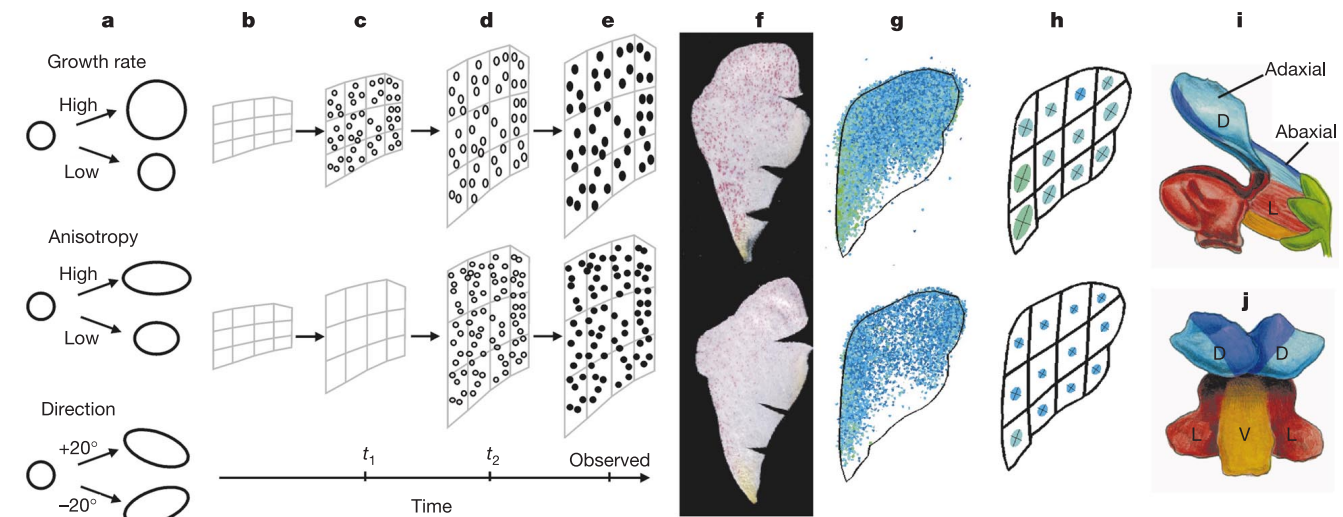


Figure 1 Determining growth parameters. **a**, Growth parameters responsible for regional shape changes, illustrated by the deformations of a growing circle. Growth rate affects area, anisotropy affects stretch and direction determines the angle of the stretch. **b–e**, Estimating growth parameters from clones. Clones are induced in a growing organ at two different developmental times, t_1 (top) and t_2 (bottom), in parallel experiments. By comparing the average characteristics (areas, shapes, directions) of the clones resulting from the two experiments (that is, by comparing the top and bottom of **e**), growth parameters for each region can be estimated for the (t_1, t_2) time interval. **f–h**, Gathering clonal data from *Antirrhinum* petals. Top and bottom show information from clones induced at P44 and P46 respectively. Clones were generated using an unstable *PALLIDA* (*PAL*) allele that carries a temperature-sensitive transposon²⁹. Transposon excision can be induced at specific times in a proportion of cells by switching plants grown at 25 °C to

15 °C for a short period³⁰. This treatment has no obvious effect on petal shape. Excision restores *PAL* gene function, resulting in clones of red epidermal cells in mature petals (**f**). For each induction time, clones from 23 flattened dorsal petal lobes on average were imaged and mapped onto an average petal shape (**g**) (A.-G. R.-L., S. J. Impey, E.C. and J.A.B., manuscript in preparation). Colour reflects clone size (blue is smaller than green). Average clone characteristics for different regions were computed for inductive time points separated by two plastochrons (**h**). For clarity, ellipse areas are scaled up by a factor of 20 relative to the petal size. Data from abaxial and adaxial lobe surfaces were treated separately. **i–j**, *Antirrhinum* flower, side (**i**), and face (**j**) view. Petals are colour-coded blue for dorsal (D), red for lateral (L) and yellow for ventral (V). The most dorsal half of the dorsal petal is shown in darker blue.

shape of the organ shortly before growth arrest. By repeating this procedure for earlier and earlier intervals, while aligning growth directions with respect to the revised grids, corresponding organ shapes and grids can be computed for earlier stages. The method assumes that clones are not dispersed during growth by cell movement, a reasonable assumption in the case of plants, where cells are usually fixed relative to each other.

This method was applied to petal development in *Antirrhinum*, a

well-characterized molecular genetic system for which a key question is how petal asymmetry emerges^{16–19}. *Antirrhinum* flowers have five petals, which are united in their proximal regions to form a tube while their distal regions form five distinct lobes (Fig. 1i, j). Dorsal and lateral petals are asymmetric, whereas the ventral petal is bilaterally symmetric. Petals are about seven cells thick, and the epidermal layer has been shown to make a major contribution to overall shape^{20–22}. Most epidermal cell divisions give daughter cells in the same layer²³. Floral meristems are generated from the apex at regular time intervals (10 h in this study), termed plastochrons²⁴. Petal primordia first emerge around P18 (plastochron 18) and reach maturity at P57 (Vincent, C. *et al.*, manuscript in preparation). Cell divisions mostly stop after P46 and further growth, resulting from cell expansion, has little impact on changes in petal shape (A.-G.R.-L. *et al.*, manuscript in preparation). In this study we computed growth of the dorsal petal lobe from P32 to P46 on the basis of the analysis of epidermal clones at maturity (Fig. 1f–h and Fig. 2a–c).

The growth rate was relatively constant, with an average doubling time of 21 h over about seven rounds of cell division. The average anisotropy was 1.15 (that is, 15% more cell divisions along the principal than in the minor direction of growth per doubling time). Although it is close to isotropic growth (1.0), the anisotropy is continuously maintained and therefore accumulates to generate a stretch in overall shape. The main growth direction was relatively uniform between regions at each stage but gradually rotated during development relative to the base of the lobe. The resulting deformation meant that clones growing at -76° (positive = clockwise) to the base of the lobe at P32 ended up with an orientation of -35° at maturity.

The results were validated in various ways. First, similar changes in shape were obtained for abaxial and adaxial surfaces, representing two independent data sets (Fig. 2b, c). Second, comparison of the shape inferred from the model with SEM (scanning electron micrographs) of a P32 lobe showed that the overall shapes were similar (Fig. 2d). Third, the changes in petal area calculated from the model were consistent with those obtained by directly measuring areas (Fig. 2e).

The pattern of cell shapes at P32 was also examined, using three-dimensional (3D) reconstructions to account for any effects of curvature⁶ (Fig. 2f). Cells were mainly elongated perpendicular to the base of the lobes (Fig. 2g). Cell wall orientations, which reflect the history of cell division planes²⁵, were most frequently perpendicular or at right angles to the base of the lobe (Fig. 2g). Thus, cells were axialized in a direction similar to the growth direction at P32 inferred from clonal analysis (Fig. 2b). This suggests that the directionality of growth depends on cell populations expanding and dividing preferentially in a given direction. By contrast, cell divisions in *Drosophila* wing development are thought to be

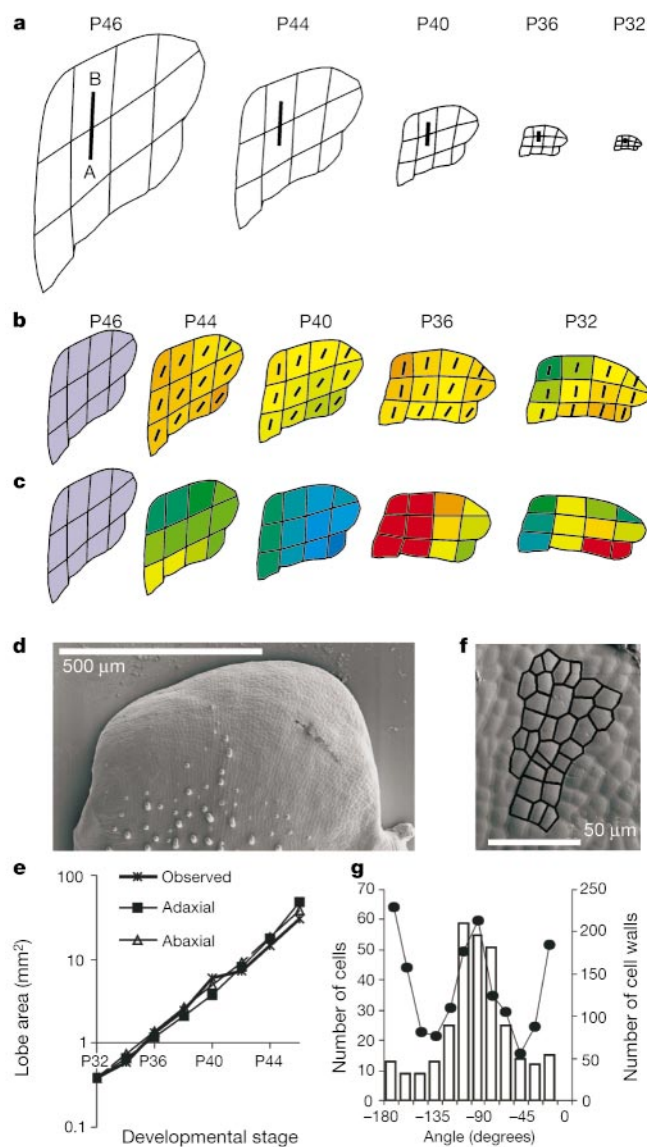


Figure 2 Results and validation of growth analysis. **a**, Changes in the shape, size and grid of the dorsal petal lobe from P46 to P32 based on changes in clones (not all stages are shown). Growth directions are computed relative to AB. **b**, **c**, Shapes as in **a** but scaled to the same size showing results for abaxial (**b**) and adaxial (**c**) data. The mature shape (P46) is shown in lilac. In **b**, the main growth direction is shown at the centre of each region and colour-coding refers to growth rate, which ranges from a doubling time of 15 h (orange) to 45 h (dark blue). In **c**, colour-coding refers to anisotropy (ratio of the increase along the main growth direction to the increase along the direction perpendicular to this, each time cell number doubles), which ranges from 1.04 (blue) to 1.5 (≥ 1.3 is red). **d**, Scanning electron micrograph (SEM) of a dorsal petal at P32. Scale bar, 500 μ m. **e**, Change in area from P32 to P46 based on the growth model compared to that based on direct measurements of petal lobes. **f**, Cell outlines on an SEM of a petal lobe at P32. Scale bar, 50 μ m. **g**, Distribution of angles of the main cell axis (bars) or cell walls (closed circles) relative to the base of the lobe, based on ten SEMs.

Doubling time	Obs.	21 h	21 h	21 h	Obs.	Obs.
Anisotropy	Obs.	Obs.	1.15	1.15	1.3	Obs.
Direction	Obs.	Obs.	Obs.	19.5°	Obs.	0°

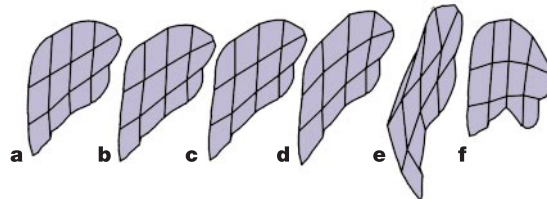


Figure 3 Petal lobe shapes at P46 resulting from growth simulations run forwards in developmental time from P32. **a**, Simulation incorporates observed (Obs.) growth parameters. **b**, Growth rate is set to its average over space and time. **c**, Growth rate and anisotropy are set to their average. **d**, All three growth parameters are set to their average. **e**, Anisotropy is set to 1.3. **f**, Growth direction is set parallel to AB in Fig. 2a.

randomly oriented, with directionality arising postmitotically¹⁴.

The contributions of growth parameters to final shape were explored by running the model forward in developmental time (Fig. 3a). To determine whether the asymmetry in petal shape reflects differential growth rates, a simulation was run with growth rate set to its average over space and time. This generated an asymmetric final petal shape roughly similar to the mature petal, showing that heterogeneity in growth rates was not critical (Fig. 3b). Further simulations showed that the asymmetry of the petal depended largely on the overall direction of anisotropic growth (Fig. 3c, d). The amount of anisotropy determined the extent to which the petal was stretched while the principal growth direction determined petal asymmetry (Fig. 3e, f). These transformations can be compared to oblique stretches of the kind proposed by Thompson²⁶ to describe the relationship between different biological forms, although he used them mainly as a static measure rather than in the dynamic developmental sense used here.

The base of the lobe, which corresponds to the boundary between lobe and tube (Fig. 4a), turns through an angle of about 45° during development as the tube grows more on its dorsal side (Fig. 4b–d). If this is taken into account and the petal lobes are oriented relative to the flower as a whole, it becomes evident that the growth direction is maintained roughly parallel to the proximodistal axis throughout development (Fig. 4e). This suggests that a long-range signal

(arrows in Fig. 4b–d) acts continuously during development to maintain the growth direction along the proximodistal axis of the petal as a whole. Long-range signals have been described before with regard to patterns^{27,28} but this is the first time one has been linked quantitatively to directional growth and the generation of shape.

On the basis of this analysis, the main transformations in petal lobe shape can be captured by the following model. Growth rates and anisotropy are fixed at 21 h and 1.15 respectively. The long-range signal is modelled by assuming that the direction of growth is fixed (vertical in Fig. 4f) while the lobe rotates through an angle of 45°. This generates a good approximation of the final shape with minimum parameter complexity.

Received 13 August 2002; accepted 20 January 2003; doi:10.1038/nature01443.

1. Avery, G. S. *Structure and development of the tobacco leaf*. *Am. J. Bot.* **20**, 565–592 (1933).
2. Richards, O. W. & Kavanagh, A. J. The analysis of the relative growth gradients and changing form of growing organisms: Illustrated by the tobacco leaf. *Am. Nat.* **77**, 385–399 (1943).
3. Erickson, R. O. Modeling of plant growth. *Annu. Rev. Plant Physiol.* **27**, 407–434 (1976).
4. Erickson, R. O. Relative elemental rates and anisotropy of growth in area: a computer programme. *J. Exp. Bot.* **17**, 390–403 (1966).
5. Wolf, S. D., Silk, W. K. & Plant, R. E. Quantitative patterns of leaf expansion—Comparison of normal and malformed leaf growth in *Vitis-Vinifera* Cv Ruby Red. *Am. J. Bot.* **73**, 832–846 (June 1986).
6. Dumais, J. & Kwiatkowska, D. Analysis of surface growth in shoot apices. *Plant J.* **31**, 229–241 (2002).
7. Hernandez, F., Havelange, A., Bernier, G. & Green, P. B. Growth behavior of single epidermal cells during flower formation: Sequential scanning electron micrographs provide kinematic patterns for *Anagallis*. *Planta* **185**, 139–147 (1991).
8. Subtelny, S. & Sussex, I. M. (eds) *The Clonal Basis of Development* (Academic, New York, 1978).
9. Poethig, R. S. & Sussex, I. M. The cellular parameters of leaf development in tobacco: a clonal analysis. *Planta* **165**, 170–184 (1985).
10. Poethig, R. S. & Szymkowiak, R. J. Clonal analysis of leaf development in maize. *Maydica* **40**, 67–76 (1995).
11. Dolan, L. & Poethig, R. S. Clonal analysis of leaf development in cotton. *Am. J. Bot.* **85**, 315–321 (1998).
12. Garcia-Bellido, A. & Merriam, J. R. Parameters of the wing imaginal disc development of *Drosophila melanogaster*. *Dev. Biol.* **24**, 61–87 (1971).
13. Gonzalez-Gaitan, M., Capdevila, M. P. & Garcia-Bellido, A. Cell proliferation patterns in the wing imaginal disc of *Drosophila*. *Mech. Dev.* **40**, 183–200 (1994).
14. Resino, J., Salama-Cohen, P. & Garcia-Bellido, A. Determining the role of patterned cell proliferation in the shape and size of the *Drosophila* wing. *Proc Natl Acad. Sci. USA* **99**, 7502–7507 (2002).
15. Poethig, R. S. Clonal analysis of cell lineage patterns in plant development. *Am. J. Bot.* **74**, 581–594 (1987).
16. Almeida, J., Rocheta, M. & Galego, L. Genetic control of flower shape in *Antirrhinum majus*. *Development* **124**, 1387–1392 (1997).
17. Luo, D. et al. Control of organ asymmetry in flowers of *Antirrhinum*. *Cell* **99**, 367–376 (1999).
18. Luo, D., Carpenter, R., Vincent, C., Copsey, L. & Coen, E. Origin of floral asymmetry in *Antirrhinum*. *Nature* **383**, 794–799 (1995).
19. Cubas, P., Lauter, N., Doebley, J. & Coen, E. The TCP domain: a motif found in proteins regulating plant growth and development. *Plant J.* **18**, 215–222 (1999).
20. Vincent, C. A., Carpenter, C. & Coen, E. S. *Plant J.* **33**, 1–10 (2003).
21. Perbal, M. C., Haughn, G., Saedler, H. & Schwarz-Sommer, Z. Non-cell-autonomous function of the *Antirrhinum* floral homeotic proteins DEFICIENS and GLOBOSA is exerted by their polar cell-to-cell trafficking. *Development* **122**, 3433–3441 (1996).
22. Efremova, N. et al. Epidermal control of floral organ identity by class B homeotic genes in *Antirrhinum* and *Arabidopsis*. *Development* **14**, 2661–2671 (2001).
23. Tilney-Basset, R. A. E. *Plant Chimeras* (Edward Arnolds, London, 1986).
24. Maksymowych, R. *Analysis of Leaf Development* Developmental and cell biology series 1 (Cambridge Univ. Press, London, 1973).
25. Lloyd, C. W. & Traas, J. A. The role of F-actin in determining the division plane of carrot suspension cells—drug studies. *Development* **102**, 211–221 (1988).
26. Thompson, D. A. W. *On Growth and Form*, 2nd edn Vol. 2 (Cambridge Univ. Press, Cambridge, UK, 1942).
27. Sachs, T. in *Pattern Formation in Plant Tissues* (eds Barlow, P. W., Bray, D., Green, P. B. & Slack, J. M. W.) (Cambridge Univ. Press, Cambridge, UK, 1991).
28. Teleman, A., Strigini, M. & Cohen, S. M. Shaping morphogen gradients. *Cell* **105**, 559–562 (2001).
29. Vincent, C. A., Carpenter, R. & Coen, E. S. Cell lineage patterns and homeotic gene activity during *Antirrhinum* flower development. *Curr. Biol.* **5**, 1449–1457 (1995).
30. Harrison, B. J. & Fincham, J. R. S. Instability at the *Pal* locus in *Antirrhinum Majus*. I. Effects of environment on frequencies of somatic and germinal mutation. *Heredity* **19**, 237–258 (1964).

Acknowledgements We thank R. Carpenter for providing plant stocks, C. Vincent and K. Lee for the scanning electron microscopy, J. Dumais for help with SEM 3D reconstructions, N. Orme for drawings in Fig. 1, S. J. Impey for gathering the image database and for early work on the project, supported by a BBSRC grant. A.-G. R.-L. was supported by a Norwich Research Park studentship.

Competing interests statement The authors declare that they have no competing financial interests.

Correspondence and requests for materials should be addressed to E.C. (e-mail: Enrico.Coen@bbsrc.ac.uk).

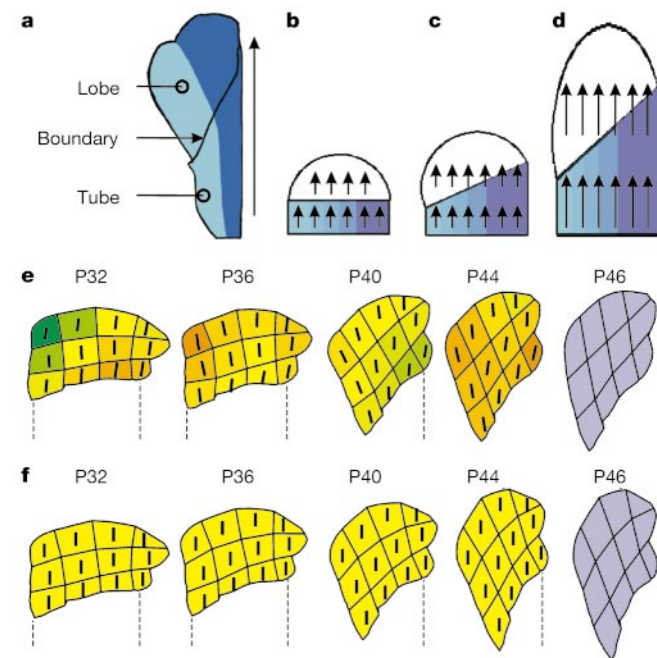


Figure 4 Growth of petal lobe in relation to the whole flower. **a**, Flattened dorsal petal colour-coded as in Fig. 1i, j, showing the boundary between tube and lobe. Arrow indicates the proximodistal axis. **b–d**, Diagram showing the change in shape from P32 to maturity when the growth direction is continuously coordinated along the whole petal by a long-range signal (arrows, arbitrarily shown pointing up rather than down). Lobe is white and tube is blue, with dorsal regions in darker blue. Initially, the lobe is bilaterally symmetrical and the tube–lobe boundary is perpendicular to the proximodistal axis of the petal (**b**). The dorsal side of the tube grows preferentially, resulting in a change in the orientation of the tube–lobe boundary (**c**). As the growth direction is maintained parallel to the proximodistal axis, anisotropic growth results in the lobe becoming asymmetric (**d**). **e**, Observed growth directions are mainly parallel to the proximodistal axis when the shapes are oriented relative to the tube (shown as dotted lines). **f**, Minimal model. Growth rates and anisotropy are fixed at 21 h and 1.15 respectively. The long-range signal is modelled by assuming that the growth direction is fixed while the lobe rotates through an angle of 45°.